Mon. Not. R. Astron. Soc. **000**, 1–15 (1999) Printed 1 February 2008 (MN LaTeX style file v1.4)

arXiv:astro-ph/0003006v1 1 Mar 2000

Bulges

Mercedes Mollá [1,3], Federico Ferrini [2] and Giacomo Gozzi [2]
[1] *Departement de Fisique, Université Laval, Chemin St-Foy, Quebec, Canadá*
[2] *Dipartimento di Fisica, Università di Pisa, Piazza Torricelli 2, 56100 Pisa, Italy*
[3] *Present address Departamento de Física Teórica, C-XI, Universidad Autónoma de Madrid, Cantoblanco 28049, Madrid, Spain*

Accepted .... 1999. Received .... 1999 ; in original form 1999

ABSTRACT

We model the evolution of the galactic bulge and of the bulges of a selected sample of external spiral galaxies, via the multiphase multizone evolution model. We address a few questions concerning the role of the bulges within galactic evolution schemes and the properties of bulge stellar populations. We provide solutions to the problems of chemical abundances and spectral indices, the two main observational constraints to bulge structure.

Key words: Galaxies: bulges – Milky Way: evolution – Spiral galaxies – Abundances – Chemical Evolution – Spectroscopic indices – Stellar Populations —

1 INTRODUCTION

Bulges are the spheroidal component of spiral galaxies. Models for their formation and evolution have been dominated in the past by the strong parallelism with elliptical galaxies, since several studies on Galactic bulge stars (e.g. Whitford 1978; Frogel & Whitford 1987; Rich 1988: Frogel 1988) claimed that their photometric properties were analogous to early-type galaxies and only old and super-solar metal rich stellar populations seemed to exist in bulges. Recently, younger stars were found in Baade's window (BW, Holtzman et al. 1993), suggesting a star formation history different from the one attributed to elliptical galaxies, i.e. strongly concentrated in the early evolutionary stages and turned off after the first Gyr. Chemical abundances in the Galactic bulge have been revised (McWilliam & Rich 1994; Minniti et al. 1995; Ibata & Gilmore 1995a, 1995b; Houdashelt 1996; Frogel, Tiede & Kuchinski 1999, hereinafter FTK99) and at present the iron relative abundance peaks at ~ -0.3 dex. A similar result has been obtained by Bacells & Peletier (1994) and deJong (1996a,b) for external spirals, by estimating from new photometric data a sub-solar mean metallicity $<$ [Fe/H] $>\sim -0.2, -0.3$ dex, suggesting that all bulges are very similar in colors and metallicities. Kinematic observations show that bulges are rotating much more rapidly than the bright elliptical galaxies, suggesting that bulges are supported by rotation at variance to ellipticals.

The main scenarios of spiral galaxies formation constraint the bulge formation: in the dissipative collapse model by Eggen, Lynden–Bell & Sandage (ELS, 1962) the evolution proceeds inwards and metallicity, age and kinematics are correlated. Zinn (1985) proposed a merger scenario, with a halo formed by accretion of small fragments, justifying the absence of a metallicity gradient in the halo. The correlation of bulge and disc scale lengths and the similarity of inner disc and outer bulge metallicities stimulated alternative models, such as a bar producing a concentration of stars in the center (Pfenninger & Norman 1990; Pfenninger & Friedli 1991) or a nuclear starburst ejecting a giant gas bubble from which stars form (Wada, Habe & Sofue, 1995). Wyse (1999) demonstrates that instabilities of purely stellar discs cannot form bulges and that the metallicity distribution in MWG is not consistent with a bulge built up from accretion of satellite galaxies or clusters.

The ELS scenario seems to recover, supported also by recent observations (Minniti, 1996a,b), and it suggests that the bulge formed through a dissipative collapse, resulting younger than the halo; FTK99 with IR data show that the metallicity presents a strong radial gradient in the inner bulge ($<$ 1.5 kpc), in agreement with previous studies (Terndrup, Frogel & Whitford, 1990; 1991 and Minniti et al., 1995). Zinn (1993) found that the inner old halo clusters (R $<$ 6 kpc) show the signature of the dissipation, and that there is a smooth transition from the halo to the disc globular clusters, suggesting that they proceed from the same collapse. Within this revival of the dissipative collapse, Van den Bosch (1998, 1999) and Elmegreen (1999) discussed the bulge formation as due to baryonic material from halo or protogalaxy settling in the center of the spheroid in a short time. The natural trend is to form a bulge because the angular momentum is low in the center, and it results older than the stellar disc. In particular, Elmegreen evaluates the threshold density for the star formation in turbulent conditions due to the gas accretion to form the bulge: a starburst phase is established in a short time scale. In both cases, the

© 1999 RAS

formation and evolution of bulges are different from elliptical galaxies.

In the present paper we wish to address the following questions; a few have already challenged the modelers and others have not been previously discussed in the literature:

- Is it needed to require the merging and/or accretion of external material to reproduce the main observed characteristics of bulges?
- Is it possible to reproduce the observed properties of bulge stellar populations?
- How far goes the analogy with elliptical galaxies?
- Which are the ages of bulges within the whole galactic evolution?

To afford these questions, we adopt the multiphase evolution model, which assumes a dissipative collapse of the gas from a protogalaxy or halo to form the bulge and the disc, in ELS scenario. The model has been applied successfully to the Galaxy and external galaxies (see papers by Ferrini and coworkers).

Mollá & Ferrini 1995 (hereinafter MF) applied first the multiphase model to study the evolution of the Galactic Bulge, considering it as a natural extension of the disc, anyway with a separate evolution: supernovae winds and no radial flows from the disc were assumed. At variance with other models present in the literature, MF succeeded in reproducing the metallicity data, revised at that date by McWilliam & Rich (1994). In the present approach, first we modify the modeling of the bulge, by considering a core population in the central region. In this scenario, the nuclear population is distinguishable from the bulge one as far as metallicity and dynamics are concerned: nuclear starts are more metal–rich and have higher α elements abundances. Furthermore, their motion must be supported by rotation, as predicted by dissipative collapse models. Indications about a different kinematics of stars in the galactic nucleus come from relatively large data sets of OH/IR stars (Lindquist et al. 1992) and ordinary M giants (Blum et al. 1995) in the 5–200 pc region. These two samples appear to trace different populations: while the M giants appear to joint smoothly with the kinematics of other bulge tracers at larger radii, OH/IR stars have a lower velocity dispersion ($\sigma_{OH/IR} = 50 - 100$ km/s against $\sigma_M > 100$ km/s) and a very high rotational velocity ($V_{rot} > 100$ km/s at a distance of 100 pc from the galactic center), against an almost negligible rotation of the M giants. The OH/IR stars may be associated with the nuclear bulge star population.

We extend the discussion to a set of external galaxies, whose discs have been extensively studied by our group (Mollá, Ferrini & Diaz 1996, 1997).

The theoretical model is presented in §2; in §3 are the result of the new bulge model. In §4 we analyze the chemical evolution results for all the bulge sample, by including the study of possible trends with the galactic properties (Hubble type, total mass). In the section §5, we predict the values for the Lick spectral indices Mg$_2$ and Fe52 and compare these predictions with observational data. Discussion and conclusions are in §6.

2 THE EVOLUTION MODEL

In the multiphase approach the star formation is considered a two step process: the diffuse gas forms molecular clouds, then stars form from cloud-cloud collisions (spontaneous star formation) or by the interaction of massive stars with molecular gas which induces star formation. We discussed extensively this approach in previous papers (e.g. Ferrini et al. 1992) and fixed the relevant parameters which define the coupling between the phases and the zones. Interesting to our present paper is essentially the collapse time scale τ_{coll}, which defines the infall gas rate from the halo to the secondary disc region or bulge. We already discussed how this varies with the galactic mass and with the galactic radius (Ferrini et al. 1994). Spontaneous star formation and cloud formation rates depend on the radial distance, too, and on the Hubble type (Ferrini & Galli, 1988). The corresponding efficiencies ϵ_μ and ϵ_H will be varied according to the prescription of Ferrini et al. (1994) while induced star formation, due to the interaction of massive stars with the diffuse gas is considered as a local process, without any radial dependence, and its efficiency has the same value used in our previous disc models. Cloud formation and star formation by cloud-cloud collisions in bulge and core regions are enhanced in agreement with our previous analysis of disc zones.

In the first application of the multiphase model to the bulge region (MF), this was considered as the natural continuation of the disc, as moving radially from the Sun to the Galactic Center. Hence the parameters for star and cloud formation were calculated following their radial variation as in Ferrini et al. (1994). The first approach gave results in good agreement with observational data, showing that it does not appear necessary to invoke a merger or an accretion from extragalactic matter to explain the origin of the bulge. However, observational data show that the bulge is not the disc continuation toward the Galactic center, but it represents a distinct region, as is it apparent from IRAS and COBE results (Dwek et al. 1995). In this paper we consider the galactic bulge as a distinct region respect to the disc, formed by the infall of gas from the halo over the bulge, without appreciable exchange of gas with the disc (Wyse & Gilmore 1992). We consider that the central galactic region is formed by three distinct zones and corresponding populations: the bulge, the halo over the bulge and the core. The bulge is modeled following Kent (1992) mass model as an oblate spheroid flattened on the galactic plane with semi major axis $x = 2$ kpc, semi minor axis $z = 1.5$ kpc, and with a mass $M_B = 1.8 \times 10^{10} M_\odot$. The core has the same shape of the bulge scaled to a semi major axis of 500 pc. The three zones interact by means of gas infall toward the center and through an outflow of gas driven by supernovae (SN) winds. The time scales for collapse from halo to bulge (τ_H) and from bulge to core (τ_B) have been chosen to reproduce the correct final masses for the three zones. With this constraint, we have used the values $\tau_H = 0.7$ Gyr and $\tau_B = 10$ Gyr. The collapse time we find in this way for the halo is shorter but not very different from that found in MF by extrapolating from the value in the solar neighborhood ($\tau_H \sim 1$ Gyr). As in MF, a SN-driven wind occurs when the thermal energy produced by combined SN explosions is larger than binding energy, calculated as $E_B = GM(R)M_{gas}/R$, where $M(R)$ is the total mass within radius R.

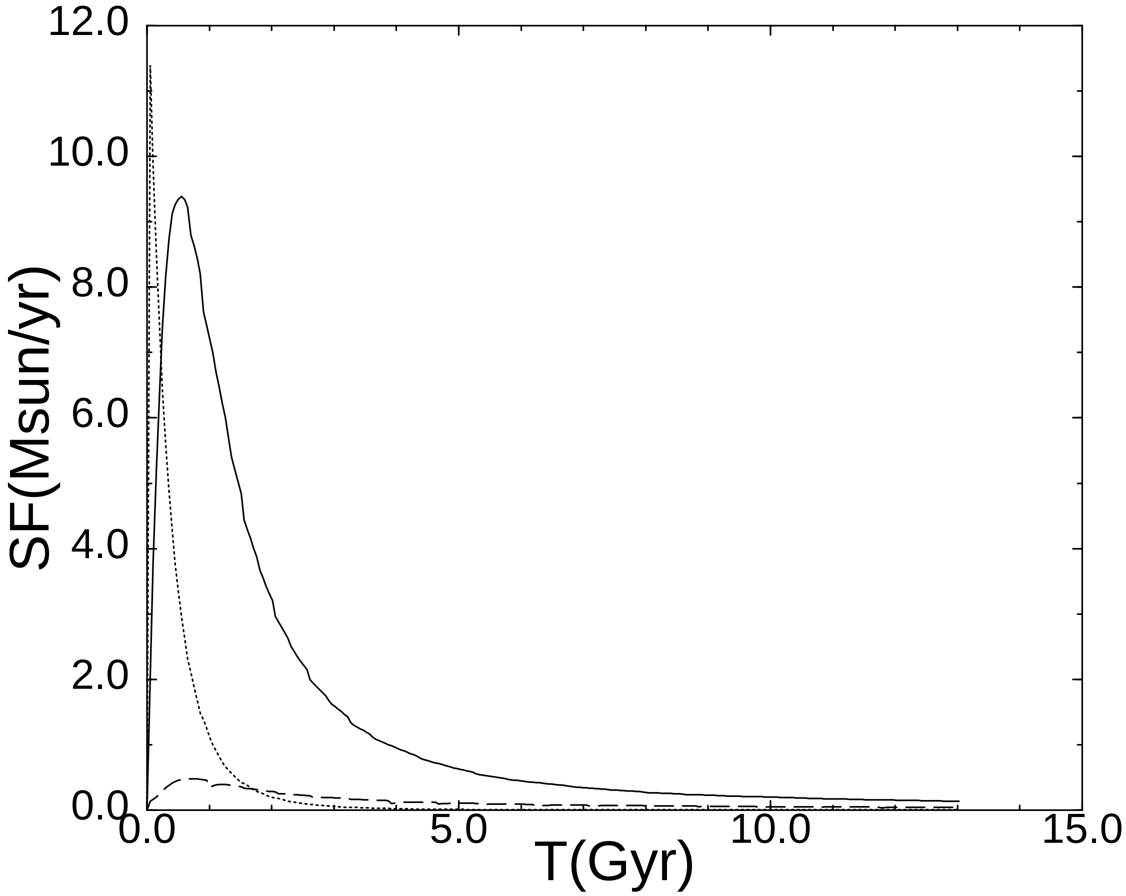

Figure 1. SFR as a function of time for the three zones: bulge (solid line), halo (dotted line) and core (long dashed line). Line styles are the same for all figures.

In comparison with MF we have updated α element nucleosynthesis from massive stars, in the mass interval $8M_\odot \leq M \leq 100M_\odot$. We use the computations of SN type II nucleosynthesis by Woosley & Weaver (1995) (WW95). WW95 calculate nucleosynthesis models for three different explosion energies and for several initial abundances. Initial abundances do not affect very much nucleosynthesis yields, while larger explosion energies increase them. We adopt their model with intermediate explosion energies (Model B) with initial solar abundances, to have a larger number of stellar masses.

The model we are going to apply to the bulges of nine external galaxies is the same used for the Galactic bulge, but simplified since we do not include the core region. We assume a protogalaxy with a sphere of primordial gas whose total mass $\mathrm{M_{tot}}$ is calculated using the rotation curve $V(R)$: $M(R) = 2.32 \times 10^5 \times V_{rot}(R)^2 \times R$ (Lequeux, 1983).

3 THE BULGE OF MILKY WAY GALAXY

3.1 Star Formation history

Figure 1 shows the Star Formation Rate (SFR) in the three zones. Star formation in the halo over the bulge is similar to the star formation in the halo over the solar region: it dominates at early times and is essentially switched off after 2 Gyr. The time scale for star formation in the bulge is longer, approximately 5 Gyr, while the maximum of star formation is reached at $t \simeq 0.6$ Gyr. According to our model there is a significant number of intermediate age (< 10 Gyr) stars in the galactic bulge, in agreement with observational data of Holtzmann et al. (1993). In the core the maximum appears at the same time, but the star formation rate reduces more slowly because of the residual infall of gas from the bulge. We can conclude that star formation starts in the external region and continues mainly toward the center after about 0.5 Gyr; the bulge formation occurred after the formation of the halo, in partial overlap with the thick disc formation and almost completely before the thin disc produces efficiently stars.

3.2 Element Abundances

Figure 2a and 2b show respectively the time evolution of iron abundance, [Fe/H] and of oxygen abundances, [O/H], for the three zones. The enrichment goes on during the collapse, then the relation steepens as the radius decreases. The halo stars are very metal poor. The average metallicity $\overline{[\mathrm{Fe/H}]} = -1.49$ is in good agreement with observational data by Zinn (1985) for halo globular clusters within a distance $R = 3$ kpc ($\overline{[\mathrm{Fe/H}]} = -1.47$).

The average metallicity $\overline{[\mathrm{Fe/H}]}$ for the bulge stars agrees

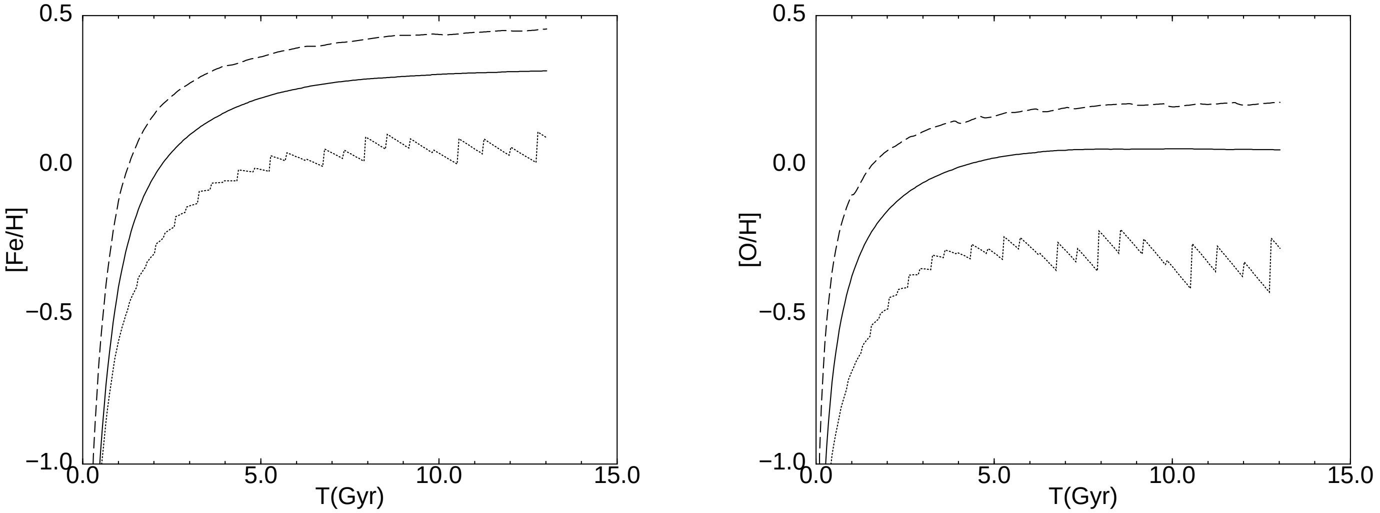

Figure 2. Time evolution of (*a*) [Fe/H] and (*b*) [O/H] for the three zones.

with the observational data by McWilliam & Rich (1994 – hereinafter McWR94) for a sample of K giants in the BW, as it will be discussed in next section.

In Table 1 we present the main features of star formation in columns 2–4: SFR at 13 Gyr (SFR$_{now}$), the ratio of maximum to present SFR (S_m/S_n), the present mass fraction in each zone. In columns 5–9 are shown the main features of gas enrichment: the time at which solar abundances are attained by iron and oxygen (t_{Fe} and t_O respectively), the present iron and oxygen abundances and the average metallicity (iron abundance).

The abundance of α elements is of particular utility to understand the formation time scale of the galactic bulge. In Figures 3a-3d we show our model results for [O/Fe], [Mg/Fe], [Ca/Fe] and [Si/Fe] versus [Fe/H] for the three zones compared with the data by McWR94 for K giants in the BW. From the Figures 3 we can see that core stars present enhanced abundances of α element compared with bulge ones. Observational data for O, Ca and Si are very well reproduced. On the contrary, our model is not able to reproduce observational abundance for Mg. The abundance ratio [Mg/Fe] found by McWR94 is enhanced by ~ 0.3 relative to solar over almost the entire [Fe/H] range. Only the two stars with the smallest [Fe/H] ratios are reproduced by our model. This underestimation is probably due to the SN II nucleosynthesis model we have used. Thomas, Greggio & Bender (1998) compare SN II nucleosynthesis models by WW95 with that of Thielemann, Nomoto & Hashimoto (1997), focusing on the [Mg/Fe] ratios; they find that the last calculation model leads to an enhancement of Mg abundance by 20 per cent relative to WW95 models. To reproduce the Mg abundance, the SN II nucleosynthesis would be two times higher than predicted by WW95 model. We can conclude that no model available today can reproduce Mg abundance observed in the bulge K stars.

Figure 4a shows the model result for Mg abundances compared with the data by Sadler, Rich & Terndrup (1996) (SRT96). The displayed data represent the average values of [Mg/Fe] computed dividing the stars sample into four bins. Model results are lower but still consistent with SRT96 observational data. In Figure 4b we shows our model results for [(C+N)/Fe] ratios versus [Fe/H] compared with SRT96 data, collected as in Figure 4a. The observational data seem well reproduced, even if the large uncertainty for abundance ratio ($\Delta_{[C+N/Fe]} = 0.4$ dex) reduces the validity of this result.

3.3 Metallicity distributions

The metallicity distribution of K giants is an important observational constraint to understand the sequential time formation of the galactic bulge. Our model gives the time evolution of the total Star Formation Rate ψ(t). To obtain the theoretical number of stars in the K giants phase from ψ(t) we used the isochrones from the FRANEC code and the Initial Mass Function adopted in this series of papers, derived by Ferrini, Palla & Penco (1990). All the isochrones correspond to an helium abundance $Y = 0.27$, according to Minniti (1996a), who finds $Y = 0.28 \pm 0.02$ with a photometric determination in the IR band of bulge stars. We used two different total metallicity: Z=0.01 for stars with age $t < 2$ Gyr and Z=0.02 for $t > 2$ Gyr. In Figure 5a-5c we show the theoretical K giants metallicity distribution for the three zones. All the distributions are normalized to unity. Moving from the halo to the core an increase of $\overline{[Fe/H]}$ and a decrease of standard deviation $\sigma_{[Fe/H]}$ are evident. In Figure 6a we present the frequency histogram of Rich (1988) solution 1 [Fe/H] corrected by the regression relation of McWilliam & Rich (1994) and the model result for the bulge region. Observations and theory agree reasonably in the range $[Fe/H] > -1.25$. For lower iron abundances the model predicts too many stars, as it happens with the G dwarf problem in the solar region. Pardi, Ferrini & Matteucci (1995) take into account the effect of the thick disc in the Galactic evolution; the presence of the this intermediate phase of accretion to the thin disc allows the solution of the

Table 1. SFR and metal enrichment

	SFR$_n$ $M_\odot/yr$	S_m/S_n	Mass %	t_{Fe} Gyr	t_O Gyr	[Fe/H]$_n$	[O/H]$_n$	$\overline{\text{[Fe/H]}}$
halo	7×10^{-4}	1.6×10^{4}	10	4.5	–	0.00	−0.30	−1.49
bulge	0.13	70	83	2.0	4.1	+0.30	+0.05	−0.26
core	0.04	15	7	1.2	1.5	+0.45	+0.20	+0.22

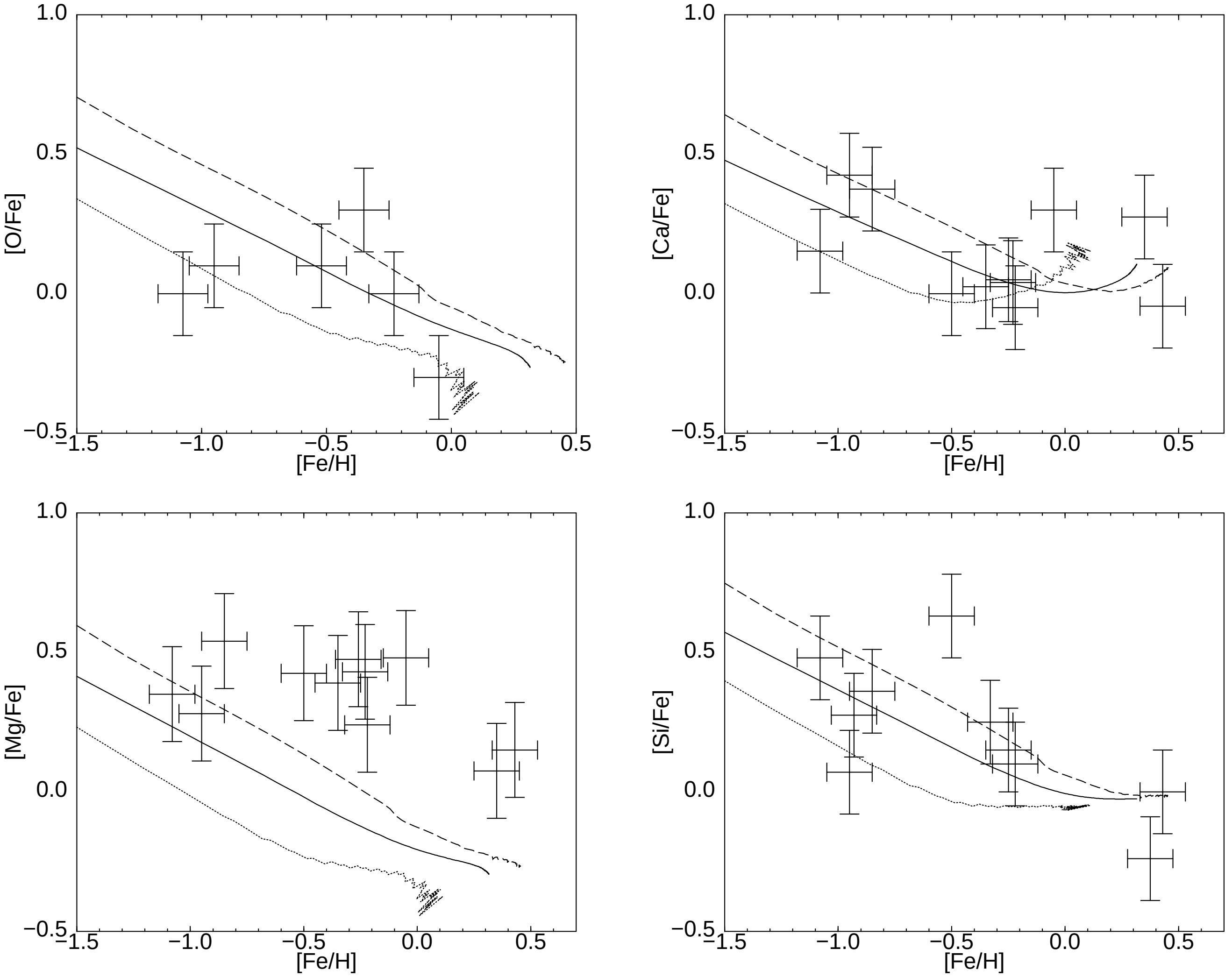

Figure 3. [α/Fe] versus [Fe/H] for the three zones. (*a*) oxygen, (*b*) magnesium, (*c*) calcium (*d*) silicon. Data are from Mc William & Rich (1994).

G dwarf problem. We may easily imagine that the introduction of a similar intermediate zone modifies the theoretical distribution on the low metallicity end.

By comparing McWR94 observational data with theoretical bulge K giants distribution of metallicity, we consider implicitly that every star in BW belongs to the bulge population, without contaminations from halo and core populations. There are anyway indications of the existence of a contribution of halo star population in the BW: Rich (1990) finds a correlation between kinematics and metallicity in a sample of K giants in the BW: giants with [Fe/H] < -0.3 have higher velocity dispersion than giants with

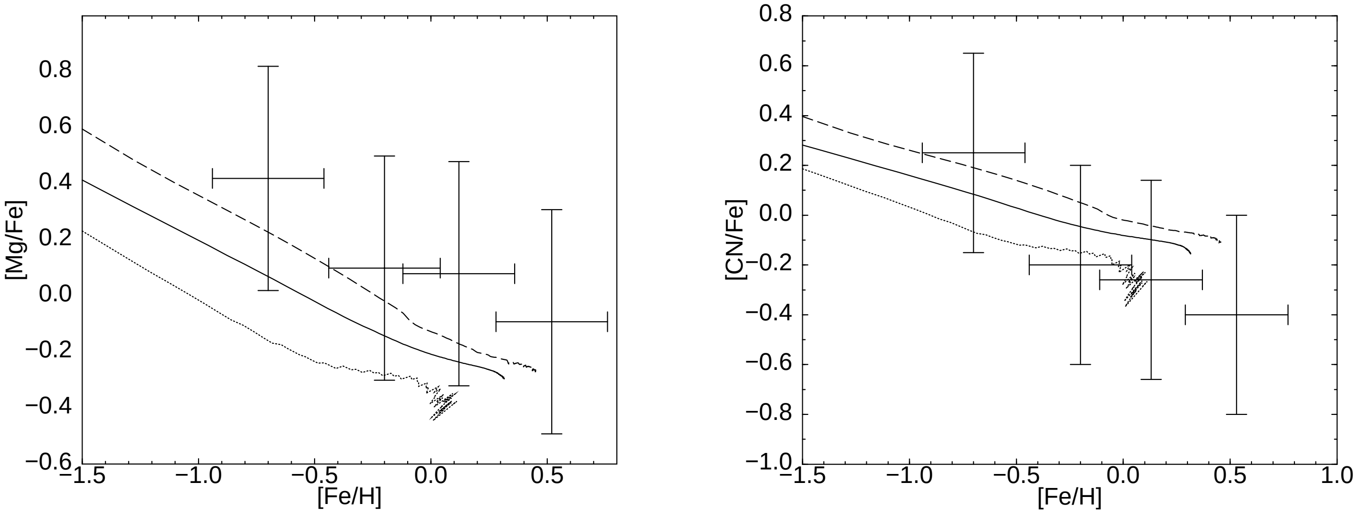

Figure 4. [Mg/Fe] (*a*) and (*b*) [C+N/Fe] versus [Fe/H] for the three zones. Data are from SRT96.

Table 2. K giants distributions: mean metallicity and standard deviations

	$\overline{\mathrm{[Fe/H]}}$	$\sigma_{\mathrm{[Fe/H]}}$
halo	− 1.60	0.85
bulge	− 0.52	0.65
core	− 0.07	0.45
comb. 1	− 0.47	0.60
comb. 2	− 0.42	0.60
comb. 3	− 0.91	0.80
comb. 1 truncated	− 0.20	0.40
comb. 2 truncated	− 0.18	0.45
McWR94 (sol. 1)	− 0.25	0.40
SRT96	− 0.11	0.45
M95 (F588)	− 0.60	0.70
M95 (M22)	− 0.60	0.70

[Fe/H]> -0.3. The velocity dispersion of the metal poor K giants is consistent with their belonging to the same $r^{-3.5}$ spheroid as globular cluster and RR Lyrae. Furthermore, in this paper we consider the existence of a third stellar population, the core one, distinct from bulge population in its metallicity distribution. With this assumption a fraction of giants in the BW, inside 550 pc from the galactic center, belongs to core population. So we can conclude that in the BW there are not only present stars belonging to the bulge population, but there must exist an overlap of the three populations.

In order to compare correctly theoretical results with observational data, we have to estimate the contributions from the different galactic components. To compute the contribution of the three stellar populations by varying the distance from Galactic Center we can use the corresponding mass distribution models. We have considered the mass model G2 of Dwek et al. (1995) for bulge star distribution; the halo star contribution has been modeled following an axisymmetric power law following Minniti et al. (1995). There are not available accurate core stars mass models; because of the stronger concentration, the contribution of core star population to the total star number can be relevant only in the BW region, up to 550 pc from the galactic center. So we have considered two combinations for the BW, differing in the core stars contribution. In combination 1, bulge stars represent 85%, halo stars 5% and core stars 10 % of the total stars. In combination 2 we have considered a larger contribution of core stars, choosing respectively 75%, 5% and 20%, for bulge, halo and core. Figure 6b shows McWR94 metallicity histogram compared with combination 1. Combination 1 better reproduces observational data, even if for iron abundances lower than [Fe/H]=-1.25 our model still predicts too many stars.

In Figures 7a and 7b, we show the metallicity distribution of pure bulge and combination 2 respectively compared with SRT96 data. SRT96 data are better reproduced by combination 2, in which core stars contribution is 20%. From Table 2 it is clear that the choice of combinations satisfies better the fitting of distributions. In Table 2 we insert also the properties of the combinations truncated to the low metallicity end, to simulate the presence of the thick disc.

Figures 8a and 8b show Minniti et al. (1995) metallicity distribution of star samples in F588 bulge field at $l, b = (8^\circ, 7^\circ)$ (8a) and in globular cluster M22 at $l, b = (8^\circ, 7^\circ)$ (8b), corresponding to distances $R = 1.5 - 1.7$ kpc from Galactic Center. Observational distributions are compared with theoretical data of combination 3 (halo stars 30%, bulge stars 70%) which corresponds in our simple scheme to these bulge regions. The observational data are well reproduced by combination 3 in the metallicity range $-2.0 \leq$[Fe/H] $\leq +0.4$. It is still present an overestimation for star with [Fe/H] ≤ -2. On the other hand the absence of theoretical stars with [Fe/H]$\geq +0.4$ can be explained considering that the scatter in the metallicity observational determinations increases for the most metal rich giants. The fact that the errors increase with metallicity to $\Delta_{[Fe/H]} = 0.4$ for the

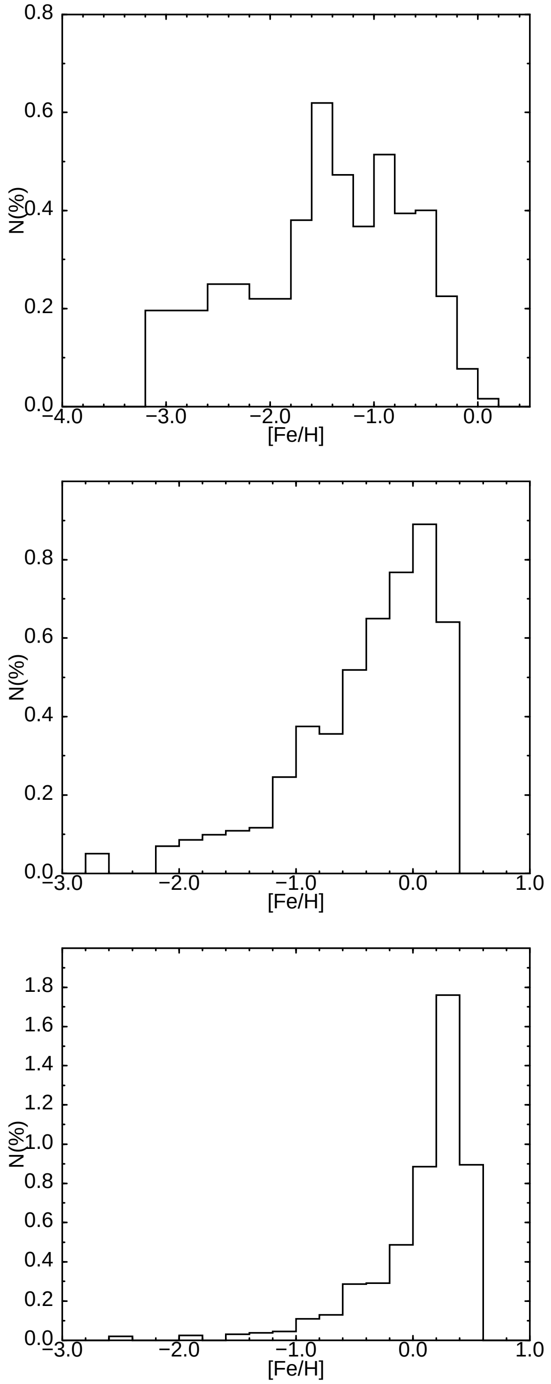

Figure 5. K giants metallicity distribution. (*a*) halo, (*b*) bulge, (*c*) core.

more metal rich stars cast doubts on the reality of the values for the most metal rich stars. Indeed, it is not clear whether there are any stars in the samples with [Fe/H]$\geq +0.5$ even in the more central zone or core (Jablonka et al. 1996; Davidge, 1998).

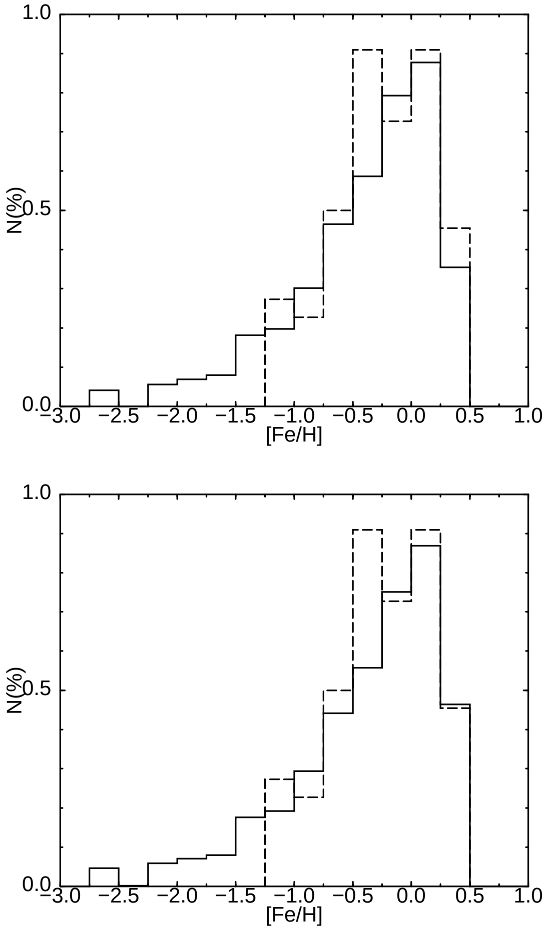

Figure 6. K giants metallicity distribution by Mc William & Rich (1994) (dashed) compared with (*a*) bulge and (*b*) combination 1 theoretical ones (solid).

3.4 Metallicity gradient

The determination of an abundance gradient in the central regions of the Milky Way is important for testing models of Galaxy formation. A metallicity gradient is predicted by dissipative collapse models. We have calculated the theoretical metallicity gradient comparing the average $\overline{\mathrm{[Fe/H]}}$ of K giants distributions at different distances from the Galactic center. We use combination 1 for giants in the BW ($R = 550$ pc) and combination 3 to reproduce giants distribution at $R = 1.5$ kpc. We find the existence of a metallicity gradient d[Fe/H]/dr $= -0.4$ dex/kpc in the bulge region ($0.5 \leq R \leq 1.5$ kpc). We have calculated the metallicity gradient in the core region with the assumption that near the Galactic center, the core star population dominates. We find the existence of a metallicity gradient d[Fe/H]/dr$= -0.8$ dex/kpc in the core region ($R < 0.5$ kpc), so that the negative metallicity gradient is not limited to the bulge region, but it continues in the core region increasing in modulus. These values are in good agreement with the value found from spectroscopy by M95 and by the new IR data from FTK99 who find a value of -0.064 ± 0.012 dex/degree for the minor axis of our Bulge.

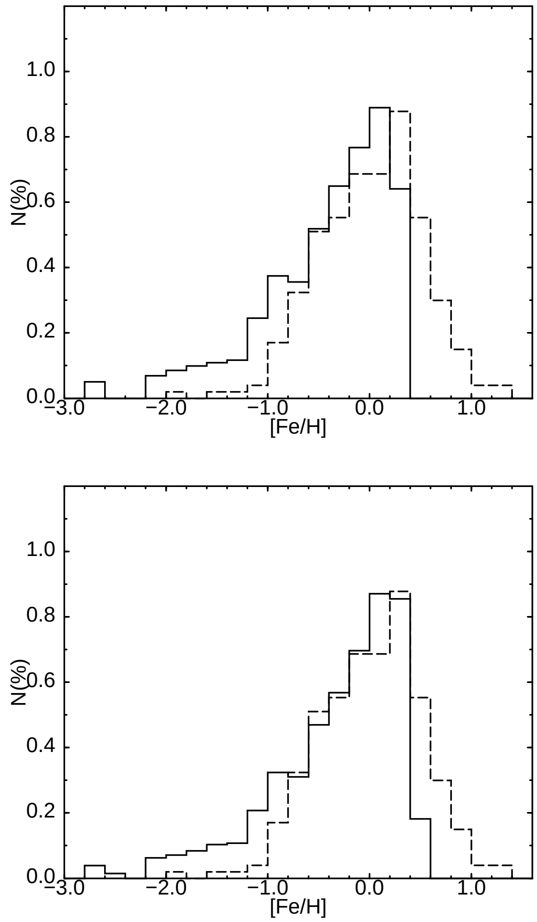

Figure 7. K giants metallicity distribution by SRT96 (dashed line) compared with (*a*) bulge and (*b*) combination 2 theoretical ones.

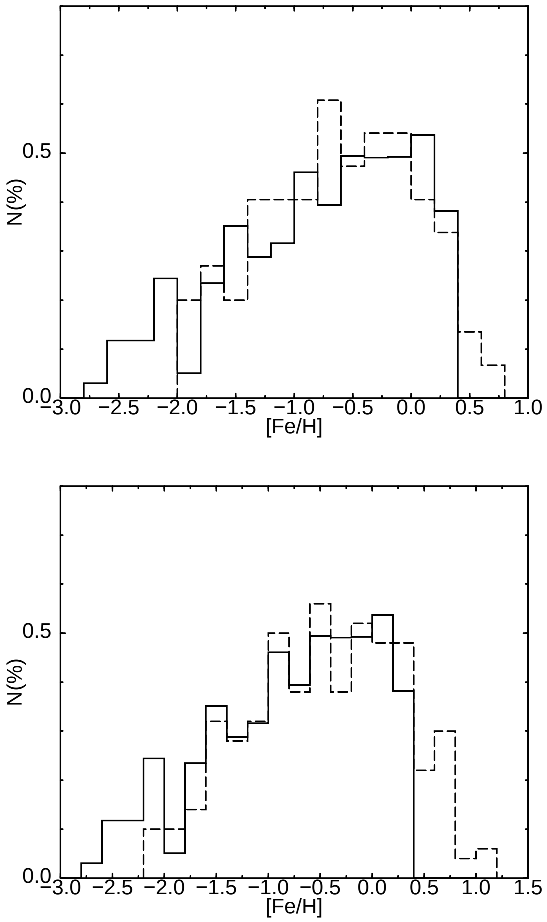

Figure 8. K giants metallicity distributions by Minniti (1995) (dashed line) compared with combination 3. (*a*) globular cluster M22, (*b*) field F588.

3.5 Gas and cloud phases

We evaluate the time evolution of atomic and molecular gas for bulge and core zones respectively. At present time atomic and molecular gas are almost in the same quantity in the bulge region, while in the core region molecular gas exceeds atomic gas as from Table 3 where we compare the total abundances for atomic and molecular gas with observational data from Sanders, Salomon & Scoville (1984) referring to the zones with distances from the Galactic center $R < 0.7$ kpc and $0.7 < R < 1.5$ kpc. The theoretical amount of molecular gas in the core region provides an underestimate to the observed quantity. On the other hand the total quantity of molecular gas estimated in both bulge and core regions together is smaller but in reasonable agreement with observational data. Our model takes into account infall of the atomic gas while molecular gas infall is not considered. The great concentration of molecular gas could only be reproduced if a similar infall parameter for the clouds in the bulge region is introduced.

We must remind that a difference intervenes however from the nature of clouds: in the bulge region, clouds have larger densities and smaller dimensions (Blitz et al. 1993) due to the gravitational potential and/or instabilities. The central half kpc region harbors a variety of phenomena unique in the whole galaxy. A number of dissipative processes lead to concentration of gas into a “Central Molecular Zone” (CMZ) of about 200 pc radius, containing $5 - 10 \times 10^7 M_\odot$ of molecular gas. In the CMZ molecular medium is characterized by large densities ($n \geq 10^4 cm^{-3}$) and a large filling factor ($f \geq 0.1$). Such densities, usually found only in the molecular clouds cores, are required to make clouds survive to tidal disruption. The clouds in CMZ also present high temperatures, in the interval 30 – 200 K, typically $\sim$ 70 K, large velocity dispersion (15–50 km/s), and apparently high magnetic fields (for a complete review see Morris & Serabyn 1996). The bar potential and the strong tidal forces may enhance clouds velocity dispersion, so that the dominant star formation process may be via relatively violent events, which cause strong compression of the already dense Galactic center clouds (Rich & Terndrup 1997).

psfile=fig9a.ps angle=270 hscale=40 vscale=40 hoffset=-20 voffset=+250

4 BULGES OF EXTERNAL GALAXIES

Table 3. Gas Phases

	H_2 ($10^7 M_\odot$)	HI ($10^7 M_\odot$)	H_2/HI
bulge	2.3	2.50	0.9
core	0.1	0.07	1.4
R< 0.7	3		
0.7 <R< 1.5	$\sim$ 1		
R< 1.5	3 - 5	0.10	50.0

Table 4. Observational characteristics.

Galaxy Name	D (Mpc)	T	Arm Class	R_{eff} (kpc)	$V_{rot,max}$ (km/s)
NGC 224	0.7	3	12	7.8	250
MWG	–	4	–	6.2	220
NGC 4303	16.8	4	9	4.6	150
NGC 4321	16.8	4	12	8.5	270
NGC 628	7.2	5	9	5.0	220
NGC 3198	9.6	5	–	4.5	160
NGC 4535	16.8	5	9	9.1	210
NGC 598	0.7	6	5	2.6	85
NGC 6946	5.7	6	9	5.1	180
NGC 300	1.6	7	5	2.4	80

Table 5. Input mass and geometry data.

Galaxy Name	R_{disc} (kpc)	R_B (kpc)	M_B ($10^9 M_\odot$)	M_{tot} ($10^{11} M_\odot$)
NGC 224	25	4.0	40	4.35
MWG	20	2.0	18	3.30
NGC 4303	14	2.0	8	1.60
NGC 4321	16	3.0	30	4.00
NGC 628	16	2.0	10	3.00
NGC 3198	12	1.5	7	1.80
NGC 4535	16	2.0	9	3.30
NGC 598	9	0.5	0.8	0.50
NGC 6946	12	1.0	6	2.25
NGC 300	7	0.1	0.1	0.45

Table 6. Model input parameters.

Galaxy Name	R_0 (kpc)	R_s (kpc)	τ_{coll} (Gyr)	ϵ_μ	ϵ_H
NGC 224	10	5.4	3	0.45	0.50
MWG	8	4.0	4	0.15	0.08
NGC 4303	6	3.0	8	0.20	0.015
NGC 4321	9	5.0	4	0.45	0.10
NGC 628	8	4.0	4	0.25	0.01
NGC 3198	4	2.7	5	0.20	0.02
NGC 4535	6	2.7	5	0.25	0.02
NGC 598	3	1.7	8	0.05	0.005
NGC 6946	5	4.5	6	0.18	0.02
NGC 300	2	1.7	15	0.07	0.007

4.1 Theoretical Models

Theoretical models have been calculated for bulges of nine spiral galaxies: NGC 224, NGC 628, NGC 3198, NGC 6946, NGC 598, NGC 300, NGC 4321, NGC 4303, and NGC 4535. These spiral galaxies have different Hubble type, implying that the corresponding bulges have different size and/or mass. Their contribution to the total light of the galaxy in the B-band is higher for early types and lower for late types. For later galaxies we will consider as *the bulge* the central region of the disc, even if it has not a clear bulge appearance.

The model we apply is the same used for the Galactic bulge and described in section 2 but with a simplification: we do not consider the presence of the core component. Features for every galaxies used in our models are summarized in Table 4. For every galaxy, named in column (1), we have: the distance D in column (2), the Hubble type T in column (3), taken from Tully (1988) and Simien & de Vaucouleurs (1986); in column (4), the arm class, taken from Elmegreen & Elmegreen (1987) and Biviano et al. (1991); in column (5) we give the effective radius of the disc R_{eff} in kpc and in column (6) the maximum rotational velocity.

The total masses are obtained from the rotation curves referenced in MFD96 for six galaxies (NGC 224, NGC 628, NGC 3198, NGC 6946, NGC 598, and NGC 300) and in MHB99 for the three Virgo galaxies NGC 4321, NGC 4303 and NGC 4535. Geometrical and mass data used as input in our models are shown in Table 5. Discs and bulges radii are in columns (2) and (3); the bulge and total masses are in columns (4) and (5).

In Table 6, model input parameters are given: column (2) solar equivalent radius R_0, column (3) disc scale length R_s, column (4) collapse time $\tau(R_0)$; columns (5) and (6) ϵ_μ and ϵ_H, efficiencies respectively for cloud formation and cloud–cloud interaction, dependent on Hubble type.

4.2 Star Formation Histories

In this section we analyze the model results for the nine studied cases of bulges or central regions, as for late type galaxies.

We start by analyzing the star formation related results, summarized in Table 7. As expected more massive and early type galaxies present a more intense initial episode of star formation, suggesting a mini–burst (see Elmegreen 1999), as shown in figure 9.

The time when the maximum of the star formation occurs –column (2) of Table 7– is approximately the same for all bulges, being between 0.4 and 0.9 Gyr, always before 1 Gyr. Logically, the absolute value maximum of the star formation rate Ψ_m, column (3), is larger for massive bulges than for those with lower total mass. Therefore, the stellar mass created in this early time step is larger for more massive bulges corresponding to earlier type galaxies. One important point is that differences between maximum and present values for the star formation rates – columns (3) and (4) of Table 6 – are much lower in panel b) than in panel a) of Figure 9. This means that the SFR is more continuous, with a more constant value in time for bulges of later type

Table 7. Bulge model results.

Galaxy Name	t_m (Gyr)	Ψ_m ($M_\odot$/yr)	Ψ_n ($M_\odot$/yr)	M_{HI} ($10^{9} M_\odot$)	M_{H_2} ($10^{9} M_\odot$)	M_s ($10^{9} M_\odot$)	M_H/M_B
NGC 224	0.40	29.2	0.38	0.30	0.30	37.50	0.05
MWG	0.60	8.6	0.22	0.19	0.20	17.87	0.09
NGC 4303	0.90	2.4	0.13	0.12	0.31	6.88	0.09
NGC 4321	0.45	17.3	0.30	0.20	0.39	27.16	0.08
NGC 628	0.75	4.1	0.14	0.09	0.44	8.83	0.07
NGC 3198	0.85	1.9	0.12	0.08	0.19	5.98	0.12
NGC 4535	0.65	3.7	0.13	0.07	0.30	8.00	0.09
NGC 598	0.75	0.15	0.02	0.01	0.03	0.03	0.50
NGC 6946	0.60	1.5	0.10	0.03	0.10	4.62	0.25
NGC 300	0.40	0.05	0.002	0.0002	0.0008	0.024	3.20

galaxies. In any case, the enhancement of star formation for the bulge bursts are not very high in comparison with higher values reached in elliptical or starburst galaxies.

The ratio between past and present values is correlated with the Hubble type or with the Arm Class, since the ratio $\Psi(m)/\Psi(n)$ varies with continuity. Indeed the morphological classification of galaxies in Hubble types is related to the bulge – disc luminosities ratio; a correlation between Hubble type and SFR in the bulge is expected due to the existent correlation between total mass and Hubble type. We quantify this relationship, that must be reproduced by coherent models of galaxy evolution.

From our model, early type galaxies have larger and more massive bulges and form a large number of stars in the first phase of the starburst that interests the bulge region. There also exist a correlation between the star formation rate in the bulge and the Arm Class of the disc; this means that the star formation of the bulge depends also on the dynamical features of the whole galaxy, as we underlined in previous papers where we analyzed the correlation of galactic model properties, their observational counterparts and the corresponding Arm Class classification scheme, viewed as directly related to large scale dynamical processes.

4.3 Gas Masses

The star formation processes consume the gas in the bulge; both phases are larger in absolute value of mass – columns (5) and (6) of Table 6 – in earlier type bulges, but this effect is due to the higher values of total mass. Taking into account geometrical effects, we calculate surface densities for atomic and molecular gas; it results that bulges of later type maintain higher values for both atomic and molecular gas surface densities: earlier bulges consumed their gas more rapidly than the later ones. The total molecular gas quantity depends on two process: the consumption to form stars and the formation of molecular clouds from diffuse gas. Indeed, the ratio H_2/HI has a peculiar behavior: it is lower for early type bulges because the molecular gas has been converted in stars, but it is also low for later bulges due to the slow process of molecular cloud formation. Only intermediate type bulges, such those with T=5 if massive enough, have high values for the ratio H_2/HI, which may results five times higher than in T=3 type. It is interesting to note that this trend is completely different for spiral discs, where observed H_2/HI quantity is larger for early type galaxies (Deveraux & Young, 1989), as also derived in MFD96. The same kind of behaviour occurs when the ratio H_2/HI is represented versus the Arm Class: only intermediate galaxies show higher proportions of molecular clouds in their bulges.

The total stellar mass of bulge stars – given in column (7) of Table 6 – is decreasing with the Hubble type. For less massive bulges the collapse lasts a longer time, and a larger proportion of mass remains in the halo zone such it can be seen in column (8). Moreover the already collapsed mass needs a longer time to form stars because the efficiencies to form clouds and stars are lower.

4.4 Gas Chemical Abundances

We summarize our results concerning heavy element abundances in Table 8. A few aspects deserve a detailed discussion; in columns (3), (4), and (5) we show oxygen and iron abundances relative to hydrogen and magnesium over iron abundances at the time of SFR maximum. Since the bulk of stars created near that time, the average abundances of the corresponding bulge populations are reasonably well described by these values. Due to the differences in the star formation histories, we could imagine a priori that every bulge has a different metallicity. However, the total abundances at the SF maximum turn out very similar for all bulges, with values $\sim Z_\odot/10$. The oxygen abundances also are very similar, around -0.60 dex, while the iron abundance is lower, approximately around -0.75 dex (it is synthesized mostly by SN Type I, exploding with a delay with respect to the main episode of SF, and a dispersion exists depending on the total mass in the bulge). Therefore the oldest stellar generation with the largest number of stars have approximately the same abundance for every bulge, independently of the Hubble type.

For the present time, we have the results of columns (5) $[O/H]_n$, (6) $[Fe/H]_n$, (7) $[Mg/Fe]_n$ and (8)Z_n. The total abundance almost reaches $Z_\odot$ in all cases with a weak correlation between Z_n and the mass of the bulge, the Hubble type or the Arm Class. However there are differences between elements. The oxygen abundance is about solar in all cases showing a saturation level for all bulges, but the iron abundance is higher for earlier Hubble types.

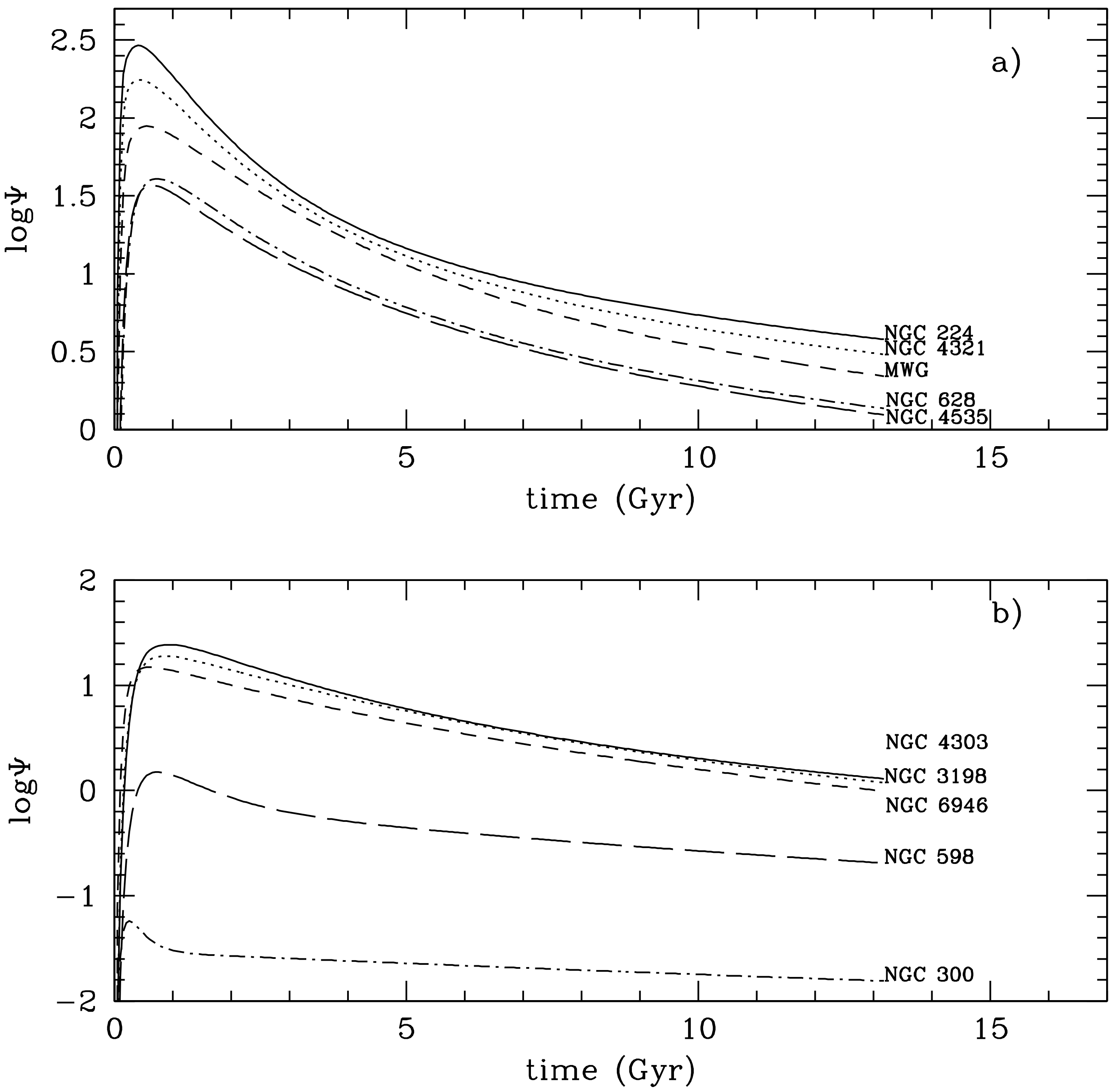

Figure 9. Star formation histories predicted for our bulge sample: a)for NGC 224, NGC 4321, MWG, NGC 618 and NGC 4535 bulges; b) NGC 4303, NGC 3198, NGC 6946, NGC 598 and NGC 300 bulges.

The average abundances for stellar populations, calculated taking into account all generations of stars are reproduced in Table 9 where column (2) is the average total abundance $\overline{Z}$, (3) average oxygen abundance $\overline{[O/H]}$, (4) average calcium abundance $\overline{[Ca/H]}$, (5) average iron abundance $\overline{[Fe/H]}$ and (6) average magnesium to iron ratio $\overline{[Mg/Fe]}$. The stellar abundances are as expected intermediate between maximum and present day gas abundances. The only possible comparison with data concerning MWG is certainly positive, since the mean stellar metallicity is $\overline{[Fe/H]} = -0.17$; this value is in agreement with the most recently estimates from FTK99, who give a value of −0.2

Table 8. Chemical Evolution Results.

Galaxy	$[O/H]_m$	$[Fe/H]_m$	$[Mg/Fe]_m$	$[O/H]_n$	$[Fe/H]_n$	$[Mg/Fe]_n$	Z_n
NGC 224	-0.61	-0.77	0.33	-0.01	0.37	-0.12	0.029
MWG	-0.54	-0.70	0.33	0.00	0.31	-0.05	0.030
NGC 4303	-0.71	-0.77	0.23	-0.02	0.27	-0.05	0.025
NGC 4321	-0.59	-0.76	0.33	0.00	0.33	-0.08	0.028
NGC 628	-0.68	-0.74	0.23	0.00	0.30	-0.06	0.023
NGC 3198	-0.61	-0.67	0.23	-0.04	0.25	-0.05	0.024
NGC 4535	-0.67	-0.71	0.34	-0.02	0.29	-0.06	0.026
NGC 598	-0.78	-0.77	0.25	-0.14	0.11	-0.03	0.019
NGC 6946	-0.47	-0.62	0.28	-0.03	0.26	-0.07	0.025
NGC 300	-0.63	-0.86	0.40	-0.12	0.11	-0.01	0.019

Table 9. Average Stellar Abundances.

Galaxy	$\overline{Z}$	$\overline{[O/H]}$	$\overline{[Ca/H]}$	$\overline{[Fe/H]}$	$\overline{[Mg/Fe]}$
NGC 224	0.015	-0.31	-0.19	-0.22	0.11
MWG	0.015	-0.29	-0.17	-0.17	0.08
NGC 4303	0.014	-0.36	-0.24	-0.24	0.07
NGC 4321	0.015	-0.30	-0.18	-0.21	0.10
NGC 628	0.013	-0.37	-0.26	-0.27	0.09
NGC 3198	0.014	-0.31	-0.19	-0.17	0.06
NGC 4535	0.014	-0.34	-0.22	-0.23	0.08
NGC 598	0.013	-0.34	-0.21	-0.20	0.06
NGC 6946	0.016	-0.24	-0.11	-0.09	0.05
NGC 300	0.016	-0.23	-0.10	-0.07	0.04

dex and also with McWilliam & Rich (1994)(-0.25 dex) and the other author's data referenced in the Introduction. Metallicities predicted for our bulges show subsolar values for the stellar populations and hence seem to exclude any similarity to massive metal-rich elliptical galaxies.

The different nucleosynthetic origin of α-elements and iron is evident in the behavior of [Mg/Fe], higher than solar for older stellar populations. In Table 7 the value reached at t_m is [Mg/Fe] ~ 0.2 dex, with a correlation with the Hubble type; [Mg/Fe] takes the highest values at t_m, while at the present time it is below solar. At t_m larger values are for earlier bulges, while at present larger values are for later bulges. The conspiracy of SF and nucleosynthesis from different populations determine the average stellar abundance to follow a smooth variation with type.

5 STELLAR POPULATIONS AND SPECTRAL INDICES

Once evaluated the global evolution of the bulge region, in particular the history of star formation, and hence the sequence of stellar generations and their corresponding element abundances, we may determine the spectral indices for the stellar populations, adopting the synthesis model results for the Single Stellar Populations (SSP). This method goes in the reverse direction of other authors (see e.g. Jablonka et al. 1996).

We use the fitting functions given by Worthey et al. (1995) to assign the spectral indices Mg_2, $H\beta$ and $< Fe >$ to each SSP, building blocks of the bulges, as functions of age and metallicity. We also assign a continuum flux, calculated with a new synthesis model developed by Mollá et al. (1999), and finally we combine all generations in the proportion determined by the created stellar mass at every time step (or at every age).

Results for the studied bulges are given in Table 10; in Figure 10 we show our predictions in the plane $Mg_2 - < Fe >$ with a set of spectral indices data observed in bulges by Jablonka et al. (1996), Idiart et al (1996a,b), Beauchamp & Hardy(1997), Vazdekis et al. (1997) and Samson et al. (1998), and the data from Gorgas et al. (1997) for low mass spheroidal galaxies. Our theoretical predictions are in agreement with the data observed in similar regions and with theoretical model for SSP obtained by Worthey (1994) and by Borges et al. (1995) and Idiart & Freitas–Pacheco (1995). Spheroidal galaxies have spectral indices very similar to those of bulges. Galaxies with large values for both indices are out of the theoretical lines, probably in agreement with larger [Mg/Fe].

First we determined the star formation and chemical evolution, then the spectral properties, as a direct consequence of both. The advantages in affording the problem with this strategy are evident in comparison with the standard analysis, based on the fitting procedure. In our study, from the first principles, late type galaxies form most stars when [Mg/Fe] has decreased in comparison with large bulges where stars are principally formed at early times, with high [Mg/Fe] values. Idiart et al. (1996b), to reproduce observations, require [Mg/Fe] values sensibly higher than ours, with [Mg/Fe] reaching 0.6 dex. Our models have a mean stellar [Mg/Fe] between 0.11 and 0.05. The multiphase model gave a mean stellar bulge metallicity $\overline{[Fe/H]} \sim -0.2$, in agreement with all recent estimations. If the statement of Peletier & Bacells (1996) that all bulges are similar in metallicities is true, our model is in agreement with them: our results of Table 9 give $\overline{Z} \sim 0.015$ and $\overline{[Fe/H]} \sim -0.20$. Idiart et al. (1996a) for the Galactic bulge require $\overline{[Fe/H]} = -0.19$, but Idiart et al. (1996b) obtain $\overline{[Fe/H]} = -0.02$ (almost solar) for the bulges of external galaxies. This difference is striking and we cannot explain why those models result so different for the Galactic bulge and the others. In our case all bulges are similar in abundances.

The spectral indices Mg_2 and $< Fe >$ show different de-

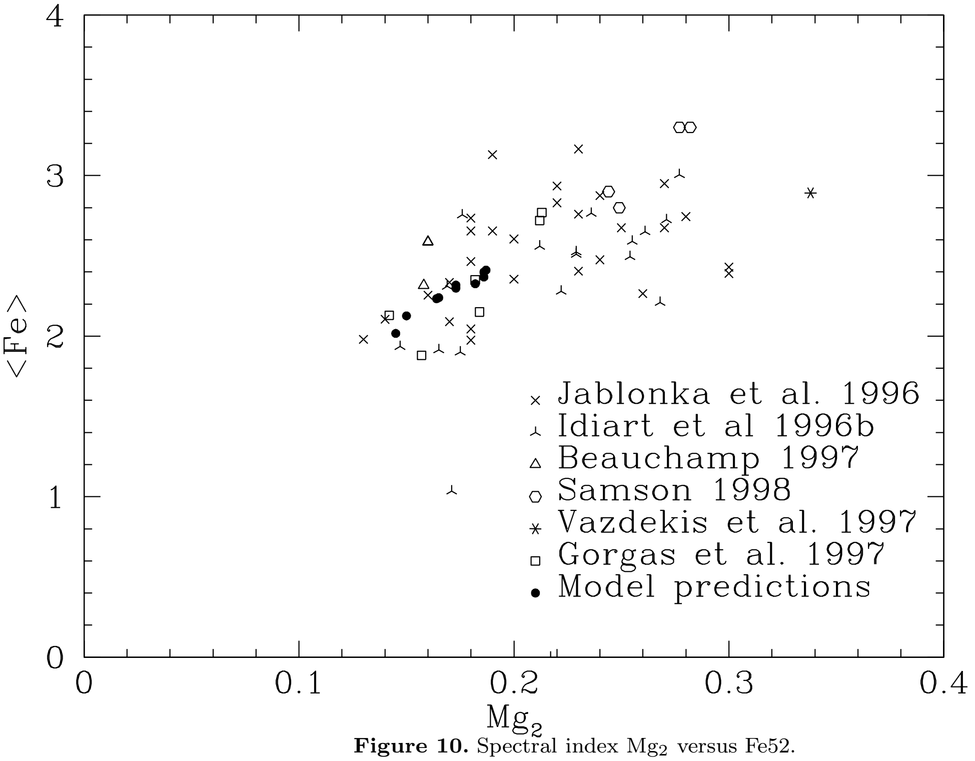

Figure 10. Spectral index Mg_2 versus Fe52.

Table 10. Predicted Spectral Indices.

Galaxy name	Mg_2 (mag)	Fe52 (Å)	Hβ (Å)
NGC 224	0.19	2.51	2.32
MWG	0.19	2.54	2.41
NGC 4303	0.16	2.36	2.45
NGC 4321	0.18	2.48	2.05
NGC 628	0.17	2.37	2.38
NGC 3198	0.17	2.43	2.70
NGC 4535	0.17	2.45	2.33
NGC 598	0.15	2.25	3.11
NGC 6946	0.19	2.54	2.14
NGC 300	0.14	2.13	3.49

pendence on the morphological type and/or the total mass of the bulge: Mg_2 depends on T while $< Fe >$ maintains constant. This results was already shown by Jablonka et al. (1996), when they represented their observed indices as a function of the luminosity M_r. The luminosity has a correlation with the mass of the bulge, which in turn depends on the total mass of the galaxy and on the morphological type. Therefore, a clear dependence between the spectral index Mg_2 and T is expected. The index $< Fe >$ does not shown any trend with T, neither with M_r. This different behavior is not explained by the different mean value [Mg/Fe], neither by differences between iron abundances in the stellar populations of different morphological types, but by the different mean ages of their populations. The earlier galaxies have old stellar populations with large magnesium abundances. Both effects increase the values of Mg_2. Later type galaxies have young populations in larger proportions. These populations have low indices and the higher proportion in mass and luminosity in the integrated quantities decrease the values of indices Mg_2. For the index $< Fe >$ the effect of the ages is the same, but iron abundances increase for later types, which produce more iron when stars are creating. Therefore, the integrated $< Fe >$ is due to a mixing of old and metal–poor stellar populations and these young populations rich in iron in the later type galaxies, while in the earlier proceed only from old stellar populations. Both effect may produce similar results, and in consequence the final $< Fe >$ does not depend on the morphological type or the total luminosity.

6 DISCUSSION AND CONCLUSIONS

The multiphase model, inserted in the dissipative collapse scenario following ELS picture, is able to reproduce the observed properties of bulges. The determination of the history of star formation as the principal ingredient of the evolution is useful in the understanding of the bulge variations in the Hubble sequence. In massive bulges corresponding to early type galaxies, the intensity of the star formation maximum is large enough to consume the whole gas, by preventing the subsequent star formation. The young stellar populations do not exist or they exist in very small proportions in comparison with the bulk of stars formed in earlier times. In later type galaxies, less massive, this maximum is not so large, and the star formation rate has almost a constant intensity. These results are in agreement with observations in the K-band from Seigar & James (1998a,b), whose results seem to indicate that the morphological types must be controlled by the star formation ratio between past and present and not by the ratio bulge/disc, because it does not present any correlation with the morphological type T.

Chemical results show bulges very similar in their abundances at the present time and for the time when the star formation maximum occurs, in agreement with estimations obtained from colors data (Peletier & Balcells, 1996; deJong, 1996a,b). Mean abundances have also been calculated by showing subsolar values and similar for all bulges independently of the Hubble type, the arm class and/or the luminosity of their host galaxies.

With a method reverse to the one adopted by Jablonka et al. (1996) and other authors, we compute the spectral indices Mg_2 and $< Fe >$ from our stellar generation results, by using SSP synthesis models. Our results are in agreement with a set of observations for bulges in the plane $Mg_2- < Fe >$. We may explain why the first of this indices depend on the Hubble type or the total luminosity of the bulge, while the index $< Fe >$ does not show a similar trend. The evolution and the star formation histories of our bulge models are crucial for this respect: the mean age of the stellar populations in bulges are different, even if the formation of the bulge himself starts at the same moment. The star formation is more continuous in the central regions of the late type galaxies than in the early type ones, by producing more iron in the stars of the first ones. This mixing of the old metal poor populations and young and iron rich populations in the late type galaxies produce the same result for $< Fe >$ than is produced by the old metal poor population created in the early type galaxies in the first phases of star formation. The magnesium is produced instead very quickly in these last galaxies, by increasing the abundance of the stars. Therefore the index Mg_2 show a clear trend with the morphological type because both ages and abundances have the same effect, by increasing the value of Mg_2.

The model shows that it is not needed the consider bars or radial flows to explain the features of bulges or their formation. Theoretical results for intermediate type bulges show the highest ratio H_2/HI. These galaxies present the strongest observed bars, as from K band data; this suggests that bars may appear and disappear in the evolution of the bulge. They would contribute to produce a new starburst phase in bulges, but it may occurs several Gyr after the formation of the bulge. In this case, the gas flows into the central region, and younger stars will be created in the bulge. Their effects would be measured if the quantity of inflow gas is large enough or comparable to the mass of stars already created in the bulge. Otherwise, their influence will be negligible in the indices Mg_2 and $< Fe >$ and we could only reveal them if we use other kind of data such the calcium triplet or $H\beta$.

We conclude presenting our answer to the questions addressed in the introduction:

- it is not needed to require the merging and/or accretion of external material to reproduce the main observed characteristics of bulges; the self–collapse of the protogalaxy seems to be sufficient to give the correct time scales, enrichment history and populations to reproduce observations not only for the Milky Way but also for external spiral galaxies.
- The observed properties of bulge stellar populations are well reproduced in detail if a correct evaluation of the contribution from the various regions involved in the bulge formation and evolution are considered, we mean the halo, bulge and core populations.
- There is no evidence of an analogy with elliptical galaxies: the apparent geometrical similarity does not correspond to any functional and physiological equivalence between these two families of astronomical objects.
- The mean age of bulges varies according to the galactic type of the parent galaxy: there is a strong correlation between the bulge populations and the whole galactic evolution.

In conclusion, not only it makes sense to figure bulge and disc evolution as two joint components of an intrinsically unitary structure, along the Hubble sequence, but it appears to be the only realistic way to obtain a good comprehension of bulge structure.

ACKNOWLEDGMENTS

M. Mollá acknowledges the Spanish *Ministerio de Educación y Cultura* for its support through a post-doctoral fellowship. F. Ferrini acknoledges the MURST for financial support. This research has made use of the NASA/IPAC Extragalactic Database (NED), which is operated by the Jet Propulsion Laboratory, Caltech, under contract with the National Aeronautics and Space Administration; the NASA's Astrophysics Data System Abstract Service; and the automated archive astro-ph, which is supported by the U. S. National Science Foundation under agreement with Los Angeles National Laboratory and by the U.S Department of Energy.

REFERENCES

Bacells, M.,Peletier, R. F., 1994, AJ, 107, 135
Beauchamp, D., Hardy, E., 1997, AJ, 113, 1666
Biviano A., Girardi, M., Giuricin, G., Mardirossian, F., Mazzetti, M., 1991, ApJ, 376, 458
Blitz, L. et al., 1993, Nature, 361, 417
Blum, R. D., 1995, ApJ, 444, L89
Borges, A. C, Idiart, T. P., de Freitas Pacheco, J. A., Thevenin, F., 1995, AJ, 110, 2408
Davidge, T. J., 1998, AJ, 115, 2374
deJong, F., 1996a, A&AS, 118, 557
deJong, F., 1996b, A&A, 313, 45
Dwek, E., Arendt, R. G., Hanser, M. G., Kelsall, T. Lisse, C. M., Moseley, S. M., Silverberg, R. F., Sodroski, T. T., Weiland, J. L., 1995, ApJ, 445, 716
Eggen, O. J., Lynden-Bell, D., Sandage, A., 1962, ApJ, 136, 749
Elmegreen, B. G., 1999, ApJ, 517, to be published on May 20
Elmegreen, D. M., Elmegreen, B. G., 1987, ApJ, 314, 3
Ferrini, F., Galli, D., 1988, A&A, 195, 27
Ferrini, F., Palla, F., Penco, U., 1990, A&A, 231, 391
Ferrini, F., Matteucci, F., Pardi, C., Penco, U., 1992, ApJ, 387, 138
Ferrini, F., Mollá, M., Pardi, M. C., Díaz, A. I., 1994, ApJ, 427, 745
Frogel, J. A., 1988, ARA&A, 26, 51
Frogel, J. A., Whitford, A. E., 1987, ApJ, 320, 199
Frogel, J. A., Tiede, G. P., Kuchinski, L. E., 1999, AJ, to be published

Gorgas, J., Pedraz, S., Guzmán, R., Cardiel, N., González, J.J., 1997, ApJ, 481, L19

Holtzmann, J. A., Light, R. M., Baum, W. A., Worthey, G., Faber, S. M., Hunter, D. A., O'Neil, E. J., Kreidi, T. J., Groth, E. J., Whestphal, J. A., 1993, AJ, 196, 1826

Houdashelt, M., 1996, PASP, 108,828

Ibata, R.A., Gilmore, G.F., 1995a, MNRAS, 275, 591

Ibata, R.A., Gilmore, G.F., 1995a, MNRAS, 275, 605

Idiart, T. P., de Freitas-Pacheco, J. A., 1995, AJ, 109, 2218

Idiart T.P., de Freitas Pacheco J.A., Costa R.D.D., 1996a, AJ, 111, 1169

Idiart T.P., de Freitas Pacheco J.A., Costa R.D.D., 1996b, AJ, 112, 2541

Jablonka, P., Martin P., Arimoto, N., 1996, AJ, 112, 1415

Kent, S. M., 1992, ApJ, 387, 181

Lequeux J., 1983, A&A, 125, 384

Lindqvist, M., Habing, H.J., Winnberg, A., 1992, A&A, 259, 118

McWilliam A., Rich R.M., 1994, APJSS, 91,749

Minitti, D., 1996a, ApJ, 459, 175

Minitti, D., 1996b, ApJ, 459,579

Minitti, D., Olszewski, E. W., Liebert, J., White, S. D., Hill, J. M., Irwin, M. J., 1995, MNRAS 277, 1293

Mollá, M., Ferrini, F., 1995, ApJ, 454,726

Mollá, M., Ferrini, F., Díaz, A. I., 1996, ApJ, 466, 668

Mollá, M., Ferrini, F., Díaz, A. I., 1997, ApJ, 475,519

Mollá, M., Hardy, E., Beauchamp, D. 1999, ApJ, 513, 695

Mollá, M. & García-Vargas, M.L. 2000, A&A, submitted

Morris, M., Serabyn, E., 1996, ARA&A, 34, 645

Pardi, M.C., Ferrini, F., Matteucci, F., 1995, ApJ, 444, 207

Peletier, R. F., Bacells, M., 1996, AJ, 111, 2238

Pfenninger, D., Friedli, D., 1991, A&A, 252, 75

Pfenninger, D., Norman, C., 1990, ApJ, 363, 391

Rich, R. M., 1988, AJ, 95, 828

Rich, R. M., 1990, ApJ, 362, 604

Rich, R. M., Terndrup, D. M., 1997, PASP, 109, 571

Sadler, E. M., Rich, R. M., Terndrup, D. M., 1996, AJ, 112, 171

Samson A. E., Proctor, R. N., Reid, N., 1998, in ASP Conf. Series No. 147 *Abunance Profiles: Diagnostic Tools for Galaxy History*, eds. D. Friedli, M. Edmunds, C. Robert, L. Drissen, 26

Sanders, D. B., Solomon, P. M., Scoville, N. Z., 1984, ApJ, 276, 182

Seigar, M. S., James, P. A., 1998a, MNRAS, 299, 672

Seigar, M. S., James, P. A., 1998b, MNRAS, 299, 685

Simien, F., de Vaucouleurs, G., 1986, ApJ, 302, 564

Terndrup, D. M., Frogel, J. A., Whitford, A. E., 1990, ApJ, 357, 453

Terndrup, D. M., Frogel, J. A., Whitford, A. E., 1991, ApJ, 378, 742

Thielemann, F. K., Nomoto, K., Hashimoto, M., 1996, ApJ, 460, 869

Thomas, D., Greggio, L., Bender, R., 1998, MNRAS, 296, 119

Tully, R. B. 1988, Nearby Galaxies Catalog (Cambridge: CUP)

van den Bosch, F. C., 1998, ApJ, 505, 601

van den Bosch, F. C., 1999, to appear in *When and How Bulges Form and Evolve*, eds. C. M. Carollo, H. C., Ferguson, R. F. G. Wyse, (Cambridge: CUP)

Vazdekis A., Peletier R.F., Beckman J.E., Casuso E., 1997, ApJS, 111, 207

Wada K., Habe A., Sofue Y., 1995, PASP, 47, 121

Whitford, A. E., 1978, ApJ, 226, 777

Worthey, G. 1994, ApJSS, 95, 107

Woosley, S. E., Weaver, T. A., 1995, ApJSS, 101, 181

Worthey G., Faber, S. M., Gonzalez, J. J., Burstein, D., 1994, ApJSS, 94, 687

Wyse R. F. G., Gilmore, G. F., 1992, AJ, 104, 144

Wyse, R. F. G., 1995, AJ, 110, 2771

Wyse, R. F. G., 1999, MNRAS, 293, 429

Zinn, R., 1985, ApJ, 293, 424

Zinn, R. 1993, in ASP Conf. Series No. 48 "The Globular Cluster-Galaxy Connection", eds. J. Brodie, G. Smith, (ASP: San Francisco), p.38

This paper has been produced using the Royal Astronomical Society/Blackwell Science LaTeX style file.